The Astrophysical Journal, 614:490–496, 2004 October 10

MATERIAL ENHANCEMENT IN PROTOPLANETARY NEBULAE BY PARTICLE DRIFT THROUGH EVAPORATION FRONTS

Jeffrey N. Cuzzi and Kevin J. Zahnle
Space Science Division, NASA Ames Research Center, MS 245-3, Moffett Field, CA 94035;
jcuzzi@mail.arc.nasa.gov, kzahnle@mail.arc.nasa.gov
Received 2004 April 5; accepted 2004 June 20

ABSTRACT

Solid material in a protoplanetary nebula is subject to vigorous redistribution processes relative to the nebula gas. Meter-sized particles drift rapidly inward near the nebula midplane, and material evaporates when the particles cross a condensation/evaporation boundary. The material cannot be removed as fast in its vapor form as it is being supplied in solid form, so its concentration increases locally by a large factor (more than an order of magnitude under nominal conditions). As time goes on, the vapor-phase enhancement propagates for long distances inside the evaporation boundary (potentially all the way into the star). Meanwhile, material is enhanced in its solid form over a characteristic length scale outside the evaporation boundary. This effect is applicable to any condensible (water, silicates, etc.). Three distinct radial enhancement/depletion regimes can be discerned by use of a simple model. Meteoritic applications include oxygen fugacity and isotopic variations, as well as isotopic homogenization in silicates. Planetary system applications include more robust enhancement of solids in Jupiter's core formation region than previously suggested. Astrophysical applications include differential, time-dependent enhancement of vapor phase CO and H_2O in the terrestrial planet regions of actively accreting protoplanetary disks.

Subject headings: accretion, accretion disks — diffusion — planetary systems: protoplanetary disks — solar system: formation — turbulence

1. INTRODUCTION

Matter does not simply condense from a cooling protoplanetary nebula at its cosmic relative abundance and remain in place. Significant inward radial transport of solids occurs relative to nebula hydrogen (Morfill & Völk 1984; Stepinski & Valageas 1997), and trace vapors migrate outward to condensation fronts (Stevenson & Lunine 1988). Each compound has its own condensation front; that of water is often called the "snow line." Previous work has stressed the role that condensation of outwardly diffused vapor plays in enhancing the density of solids at the snow line (Stevenson & Lunine 1988). However, inward particle drift can also enhance the abundance of a vapor inside the condensation/evaporation boundary (Cuzzi et al. 2003). Hence, given turbulent mixing, the density of solids just outside the boundary also grows. That particle drift can have this effect has been recognized (Morfill & Völk 1984), but the magnitude of the effect has not been recognized. Here we show that, in general, inward particle drift is more effective than outward vapor diffusion at enhancing solids outside the condensation/evaporation boundary and that in many cases of interest, vapor is also strongly enhanced *interior to* the condensation/evaporation boundary. To emphasize the difference between this new process and previous work, we often refer to the condensation/evaporation boundary as the *evaporation front*, which more accurately captures the directionality of the process described here.

In this paper we present a minimal model that illustrates the key physical arguments. We divide a condensible solid into three size classes distinguished by their transport properties: vapor and small grains that are tightly coupled to the movements of the gas, large bodies that orbit unaffected by gas drag, and midsized particles (boulders or rubble, typically on the order of a meter) that are strongly affected by both gravity and gas drag (Weidenschilling 1977). The latter can drift orders of magnitude faster than the nebula gas and carry a net flux greatly exceeding that which is coupled to the gas. The particles evaporate when they reach the evaporation front, enhancing the abundance of the condensible in the vapor phase (Cuzzi et al. 2003). While the physics is applicable to volatiles in general, we focus here on water as a volatile of special interest. The enhanced water vapor abundance spreads radially inward from the evaporation front on a timescale that is short compared to the lifetime of the nebula, potentially determining the mineralogy of primitive meteorites. Planetesimal growth just outside the condensation/evaporation boundary, or snow line, provides a sink that ultimately depletes the vapor at all locations inside the boundary (Stevenson & Lunine 1988). Ice enhancement outside the snow line can influence the location and timescale of giant planet core formation (Morfill & Völk 1984; Stevenson & Lunine 1988). Our model illustrates all these regimes of behavior.

1.1. *Nebular Evolution and Turbulence*

Protoplanetary disks evolve; both their surface mass density σ_g and mass accretion rate $\dot{M} = 2\pi R \sigma_g V_n$ (where V_n is the nebular gas advection velocity) decrease with time over a period of several million years (Calvet et al. 2000). The disk is heated by gravitational energy release ($G\dot{M}/R$) and illumination from the star. In recent models of actively accreting disks (Bell et al. 1997; Stepinski 1998; see also Woolum & Cassen 1999), midplane temperatures are hot enough in the terrestrial region to vaporize common silicates at early times and to vaporize water in the Jovian region over a more extended period. The physical cause of nebular evolution remains problematic; turbulent viscosity is now thought to face difficulties (Stone et al. 2000). However, turbulence can exist, providing

diffusivity, without necessarily providing the viscosity needed to evolve the disk (Prinn 1990; Cuzzi et al. 2001). Since diffusivity rather than viscosity is of prime interest here, we assume nebulae that are weakly turbulent. As discussed below and by Cuzzi & Weidenschilling (2004), turbulence plays several roles: it diffuses grains and vapor down concentration gradients, often against the flow of nebular drift (Cuzzi et al. 2003); it frustrates the growth of particles beyond about a meter in size; and it determines the midplane particle density (and thus the particle and planetesimal growth rates).

We presume a weakly turbulent nebula with effective viscosity $\nu_t = \alpha c H$, where c is the sound speed, H is the scale height, and the parameter α is defined by the evolutionary mass accretion rate of the nebula: $\alpha \equiv \dot{M}/3\pi\sigma_g c H$. Hence, the advection velocity $V_n = 3\alpha c H/2R$. Observations and models typically suggest that $\alpha \approx 10^{-5}$ to 10^{-2} and $H \approx R/20$. The turbulent diffusivity $\mathcal{D} = \nu_t/\mathrm{Pr}_t$ is related to the viscosity by the turbulent Prandtl number, Pr_t. It is usually presumed that $\mathrm{Pr}_t = 1$ in a turbulent nebula, but in general $\mathrm{Pr}_t \neq 1$; e.g., Prinn (1990) suggests that $\mathrm{Pr}_t \ll 1$ and that mixing is efficient even if the nebula evolves slowly. The characteristic velocity of large eddies is $V_g \sim c(\alpha/\mathrm{Pr}_t)^{1/2}$. Nebular evolution is driven by ν_t, while $\mathcal{D}$ describes mixing.

1.2. *Turbulence and Particle Growth to Meter Size*

Particle growth is easy up to meter size but problematic beyond. With or without turbulence, the relative velocities between sub–meter size particles are low, and the first aggregates probably grow by simple sticking into porous, dissipative structures (Weidenschilling & Cuzzi 1993; Cuzzi & Weidenschilling 2004). Most growth occurs as large particles sweep up smaller ones (Weidenschilling 1997). Under nonturbulent conditions, large particles sink into a high-density midplane layer in which relative velocities are low, and subsequent growth to planetesimal sizes is rapid (Weidenschilling 1997; Cuzzi et al. 1993). In turbulence, because meter-sized particles couple to the largest eddies and achieve random velocities on the order of V_g, they remain in a layer of finite thickness $h_L \sim V_g/\Omega_\mathrm{K} \sim H(\alpha/\mathrm{Pr}_t)^{1/2}$. Even weak turbulence ($\alpha > 10^{-6}$, $\mathrm{Pr}_t = 1$) keeps the density of the midplane layer and the ensuing particle growth rate substantially below their nonturbulent values (Dubrulle et al. 1995). Furthermore, meter-sized particles collide with each other at speeds comparable to V_g, meters to tens of meters per second, probably fragmenting into their smaller constituents. While particles approaching meter size, having impact strengths of 10^6 ergs cm^{-3} (Sirono & Greenberg 2000), can survive mutual collisions in turbulence of $\alpha = 10^{-4}$ (Cuzzi & Weidenschilling 2004), one suspects that further *incremental growth* may stall at the meter-size limit, at least while turbulence this large persists. Other physics, however, may come into play (e.g., Cuzzi et al. 2001). Detailed models of incremental growth, with realistic sticking and erosion based on laboratory experiments, tend to quickly produce broad power-law size distributions that contain equal mass per decade of particle radius (Weidenschilling 1997, 2000). Assuming that growth beyond the meter-size range is frustrated as described above and conservatively assuming 10 decades of particle size (microns to meters would be 6 decades), we estimate that for extended periods of time, meter-sized particles have surface mass density $\sigma_L \approx 0.1\sigma_\mathrm{sol}$, where $\sigma_\mathrm{sol} \sim 10^{-2}\sigma_g$ is the total surface mass density of solids at some location. We define $\sigma_L/\sigma_\mathrm{sol} \equiv f_L \approx 0.1$ as a key element of the model described in § 2.

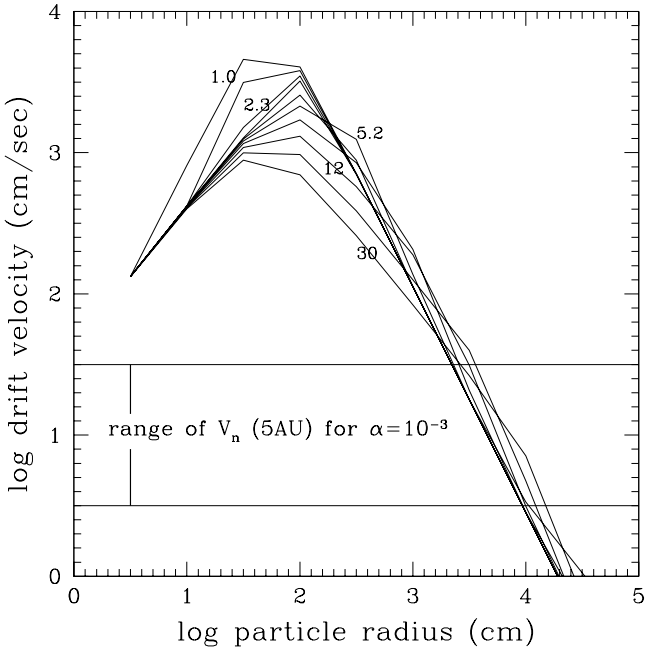

FIG. 1.—Radial drift velocity as a function of particle size, at a number of nebula locations differing by a factor of 1.5 (several labeled in AU from the star). The drift velocity at the peak is $\sim\eta V_\mathrm{K}$. For comparison, a range is shown for the nebular advection velocity V_n at $R = 5$ AU with $\alpha = 10^{-3}$ (the range is associated with different nebula density profiles; see Cuzzi et al. 2003).

1.3. *Radial Drift: Loss or Transformation?*

In general, the nebula gas has an outward pressure gradient, which counteracts solar gravity to a small degree; the ratio of these two forces is

$$\eta \approx H^2/R^2 \approx 2c^2/\gamma V_\mathrm{K}^2 \approx 2\times 10^{-3},$$

where V_K is the local Keplerian velocity (Weidenschilling 1977; Nakagawa et al. 1986; Cuzzi et al. 1993) and $\gamma = 1.4$ is the ratio of specific heats. The gas orbits more slowly than the solids at any location, and the ensuing headwind on the particles causes them to drift radially inward at velocities that depend on their size. Even weak turbulence ensures that local particle densities will be too low to affect their drift velocities (Nakagawa et al. 1986; Cuzzi & Weidenschilling 2004). Typical radial drift velocities are shown in Figure 1; they are strongly dependent on particle size but only weakly dependent on distance R from the star for nebula models such as that adopted [$\sigma_g = 1700(1\ \mathrm{AU}/R)$ g cm^{-2}]. Meter-sized particles experience the full headwind and are the most rapidly drifting; smaller particles experience a smaller headwind, and larger particles have increasing mass per unit area (Weidenschilling 1977). For comparison we show the range of gas advection velocity V_n at 5 AU and $\alpha = 10^{-3}$, which characterizes a range of radial disk density profiles. The drift velocity $V_L \approx \eta V_\mathrm{K}$ of meter-sized particles is orders of magnitude larger than V_n. It is usually inferred that such drifters are "lost into the star" on fairly short timescales; however, this is not necessarily their fate, as we describe below.

When particles drift across the location where the midplane temperature exceeds the sublimation temperature of one of their constituent species, that species will evaporate locally within distance $\Delta R \sim (m/\dot{m})V_L$, where m is the particle mass and $\dot{m}$ its evaporation rate. For water, $\Delta R < 1$ AU (Supulver

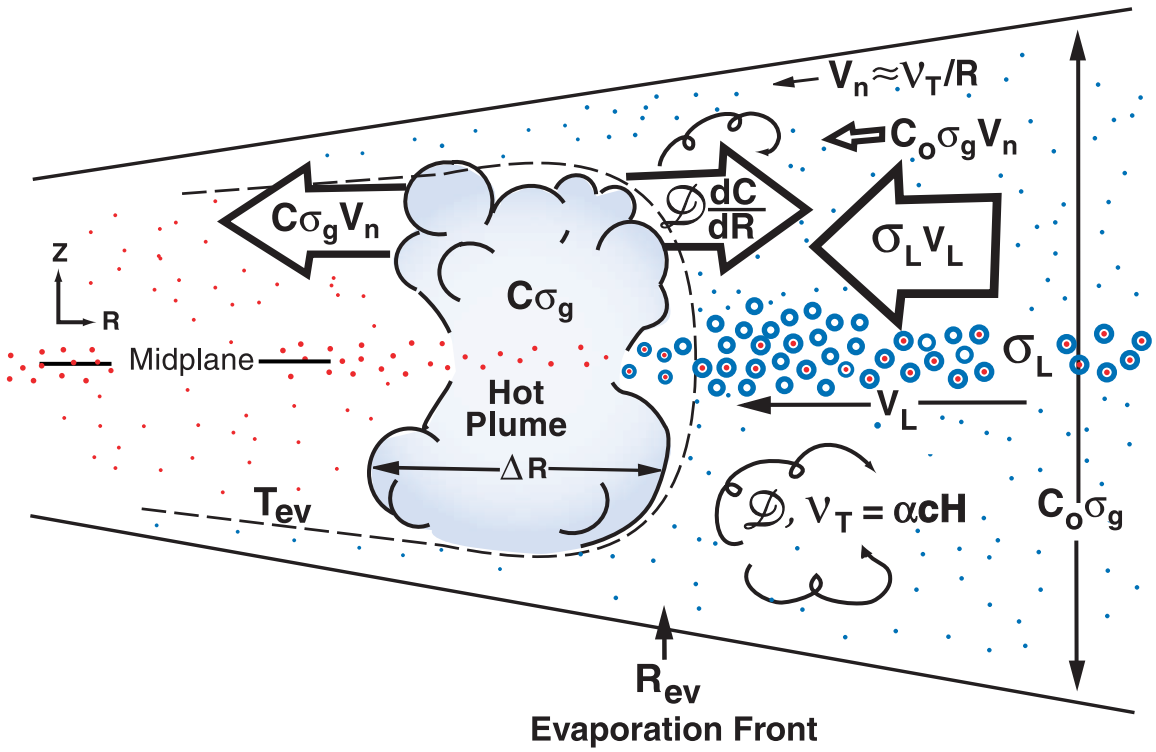

FIG. 2.—Sketch illustrating inwardly drifting volatile material (*blue circles*) crossing its evaporation front R_{ev}, with midplane temperature T_{ev}. The surface density of large midplane solids is $\sigma_L = f_L C_0 \sigma_g$; the large inward drift flux of this material, $\sigma_L V_L$, cannot be offset by vapor removal processes $C\sigma_g V_n + \mathcal{D}\sigma_g\, dC/dR$ until the concentration of the blue vapor C is much greater than the nominal solar C_0. The more refractory material (*red dots*), here shown as a minor constituent, simply continues drifting and growing.

& Lin 2000). Cyr et al. (1998) have also modeled evaporation of drifting water particles, finding that they drift considerable distances before evaporating. However, these results are incompatible with those of Supulver & Lin (2000) and with our own estimates using the same vapor pressure expressions as Cyr et al. Even after discussions with J. Lunine (2003, private communication) we cannot determine the cause of this discrepancy. For silicates, ΔR is probably larger (Cuzzi et al. 2003). This evaporation front effect can produce significant enhancement of material. We have considered only volatiles that represent significant fractions of the total condensible mass at their evaporation front: common iron-magnesium silicates, at about 1400 K (Cuzzi et al. 2003), and water ice, at about 160 K (this paper). The process is sketched in Figure 2 and described further in § 2.

1.4. *Caveats on Assumptions*

The key parameter f_L is uncertain. First, as discussed in § 1.2 and most recently by Cuzzi & Weidenschilling (2004), we believe that the actual combination of nebular turbulence α and particle strength (Sirono & Greenberg 2000) allows particles to grow to meter size. If this is not true, the appropriate value of V_L will decrease in proportion to the particle size-density product (Cuzzi & Hogan 2003). This would decrease the mass flux in "large" particles. Second, one of our simplifying assumptions was that growth is truncated above meter size and that planetesimals do not grow. This led to our estimate of f_L, the mass fraction in meter-sized particles, as simply the inverse of the number of decades of size in the "rubble" population between microns and meters. If turbulence is vanishingly small and planetesimals do grow, this simple logic loses its appeal. However, even in a planetesimal growth regime, collisional erosion or breakup will continue to occur. In this regime, f_L might be regarded as the collisionally generated, small-size end of a mass distribution with equal mass per decade, extending to 1000 km.

2. MODEL FOR EVAPORATION FRONTS

Here we construct a simplified one-dimensional model that illustrates the basic principles that govern transport of a condensible in the solar nebula. Let C represent the mobile fraction of a condensible species in the nebula. We define this as the column density of the species (vapor or solid) divided by the column density of the nebula (chiefly hydrogen and helium gas). We exclude from C material that has condensed on large planetesimals; large bodies are treated as a stationary sink.

We further subdivide C between the mass fraction f_L in fast-drifting, meter-sized rubble (§ 1.2) and the complementary fraction $1 - f_L$ in small grains (or vapor) that are strongly tied to the motions of the gas. In general, we expect that both collisional growth and disruption of particles will be faster processes than advection, so that the relative proportions of small grains to meter-sized rubble will be roughly constant where solids are stable. The evaporation front is defined by $R = R_{ev}$; inside the evaporation front $f_L = 0$. For reasons discussed in §§ 1.2 and 1.4, we assume that $f_L = 0.1$ when $R \geq R_{ev}$. Transport of C is then described by

$$\frac{\partial}{\partial t}\left[\sigma_g C(R,\ t)\right] - \frac{1}{R}\frac{\partial}{\partial R}\left[R\Phi(R,\ t)\right] = -\frac{f_L \sigma_g C}{\tau_{acc}}, \qquad (1)$$

where the inward radial mass flux Φ is the sum of nebula advection, diffusion, and particle drift, respectively:

$$\Phi = (1 - f_L) C \sigma_g V_n + \mathcal{D} \frac{\partial}{\partial R} \left[(1 - f_L) C \sigma_g \right] + f_L C \sigma_g V_L. \quad (2)$$

In equation (1) the term on the right-hand side represents the accretion sink onto large planetesimals; $\tau_{\rm acc}$ represents an accretion time. For reasons discussed above (see also Cuzzi & Weidenschilling 2004), the meter-sized particles are much more concentrated toward the midplane than smaller size ranges, which contain equal amounts of mass. We have therefore assumed that accretion onto large bodies is dominated by meter-sized particles.

2.1. *Steady State Solutions and a Likely Transient Case*

We simplify equations (1) and (2) by assuming steady state, constant coefficients, and Cartesian geometry. The latter two assumptions introduce quantitative errors on the order of unity provided that nebular properties (other than those associated with the evaporation front) vary smoothly on the scale of R, as is usually assumed in discussions of nebulae. We are left with

$$\frac{d}{dR} \left[(1 - f_L) C V_n + (1 - f_L) \mathcal{D} \frac{dC}{dR} + f_L C V_L \right] = \frac{f_L C}{\tau_{\rm acc}}, \quad (3)$$

where as before $f_L = 0$ for $R < R_{\rm ev}$.

We then further simplify equation (3) by placing all accretion onto planetesimals at the condensation front. This captures the spirit of the snow line without introducing a complete model of planetary accretion. With this simplification, equation (3) is directly solved analytically. There are four boundary conditions. At large distances $R \gg R_{\rm ev}$ the nominal cosmic abundance is $C = C_0$; i.e., $C(R \rightarrow \infty) = C_0$. At small distances $R \ll R_{\rm ev}$ there is no source of C. This precludes the purely mathematical solution in which outward diffusion balances inward advection for $R < R_{\rm ev}$. Consequently, $C(R < R_{\rm ev}) = \overline{C}$, a constant. The other two boundary conditions apply at $R_{\rm ev}$. We assume that C is continuous across $R_{\rm ev}$, and we apply a flux jump condition across $R_{\rm ev}$,

$$\Delta\Phi = \Phi(R > R_{\rm ev}) - \Phi(R < R_{\rm ev}) = \int_{R_{\rm ev} - \delta R}^{R_{\rm ev} + \delta R} \frac{f_L C \sigma_g dR}{\tau_{\rm acc}} \equiv \mathcal{L} V_n \overline{C} \sigma_g, \quad (4)$$

where $\mathcal{L}$ is a dimensionless sink factor integrated over the narrow band of planetesimals just outside of $R_{\rm ev}$, defined to make the sink term similar in form to other terms in equation (3). The steady state solution that results is

$$C(R < R_{\rm ev}) = E C_0,$$

$$C(R > R_{\rm ev}) = C_0 \left[1 + (E - 1) e^{-k(R - R_{\rm ev})} \right], \quad (5)$$

where

$$k \equiv \frac{(1 - f_L) V_n + f_L V_L}{(1 - f_L) D}, \quad (6)$$

$$E \equiv \frac{(1 - f_L) V_n + f_L V_L}{(1 + \mathcal{L}) V_n}. \quad (7)$$

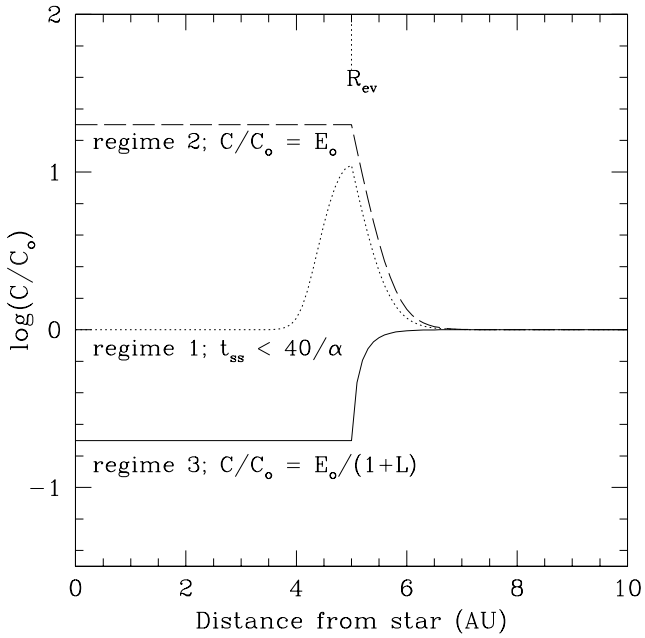

FIG. 3.—Schematic of the radial (and temporal) variation of enhancement C/C_0 for "water" with an evaporation boundary at $R_{\rm ev} = 5$ AU, taking for illustration $E_0 = 20$. In regimes 1 and 2, there is no sink at $R_{\rm ev}$ ($\mathcal{L} = 0$); regime 1 (schematic only; *dotted line*) represents the transient situation, in which the inner nebula retains $C/C_0 = 1$ for typically $40/\alpha$ orbital periods. Regime 2 (*dashed line*) is the steady state solution for $\mathcal{L} = 0$. As time proceeds and planetesimals grow in the enhanced solid density outside $R_{\rm ev}$, $\mathcal{L}$ increases; regime 3 (*solid line*) illustrates the steady state solution for $E_0 = 20$ and $\mathcal{L} = 100$.

The factor E is the enhancement over cosmic abundance. If $f_L \ll 1$,

$$E \approx \frac{1 + f_L V_L / V_n}{1 + \mathcal{L}} = \frac{E_0}{1 + \mathcal{L}}, \quad (8)$$

where the factor E_0 is that of Cuzzi et al. (2003).

In steady state the entire region interior to $R_{\rm ev}$ is enhanced over cosmic abundance (in the vapor) by the factor E. The distance scale $1/k$ is closely related to E. It is like a skin depth. It represents the distance scale beyond $R_{\rm ev}$ in which solids are enhanced. Note that if $\Pr_t < 1$, the skin depth deepens accordingly.

Enhancements can be large. Using $V_L \sim \eta V_{\rm K}$ we can estimate that, for $(f_L,\ \mathcal{L}) \ll 1$,

$$E \approx E_0 \approx \frac{f_L V_L}{V_n} \approx \frac{2 f_L}{3\alpha}, \quad (9)$$

which for $f_L = 0.1$ and $10^{-6} < \alpha < 10^{-3}$ is a very large factor indeed. By contrast, Morfill & Völk (1984) got much smaller vapor-phase enhancements (never exceeding solar) because they assumed particles that drifted only at about the same rate that their nebula was advecting ($V_L = V_n$) and because of their choice of outer boundary condition (their eq. [B7]).

We discern three regimes of interest for $C(R, t)$, shown schematically in Figure 3. Regimes 2 and 3 are the steady state solutions described by equation (5) above. In regime 2 ($\mathcal{L} \ll 1$), the entire region inward of $R_{\rm ev}$ is enhanced by E over solar. Regime 3 occurs when planetesimal growth is significant and a sink appears at $R_{\rm ev}$ ($\mathcal{L} > 1$). If $\mathcal{L}$ is big enough, the inner nebula can become depleted, essentially the result of Stevenson & Lunine (1988). Regime 1 (sketched only conceptually in Fig. 3)

TABLE 1
Interesting Ranges of Planetesimal Belt Mass and Loss Factor

α (1)	$M_{PL}/M_\oplus$ (for $\mathcal{L}=1$) (2)	$\mathcal{L}$ (for $M_{PL}=1\ M_\oplus$) (3)	$M_{PL}/\dot{M}_{PL}$, Periods (4)
10^{-6}	5×10^{-3}	200	*
10^{-5}	0.15	7	*
10^{-4}	5	0.2	200
10^{-3}	150	7×10^{-3}	6×10^{3}
10^{-2}	5×10^{3}	2×10^{-4}	2×10^{5}

Notes.—The dependence of the planetesimal accretion sink on the nebula α is illustrated in this table. In all cases, $r_{PL}=1$ km and $\xi=0.1$ are assumed. Cols. (2) and (3) are both solutions of eq. (12). Col. (2) shows that the mass of a planetesimal belt capable of providing $\mathcal{L}=1$ ranges from very small values for low α to impossibly large values for large α (a minimum mass nebula at 5 AU contains about 1 $M_\oplus$ of solids in a band of radial width H). Col. (3) shows the values of $\mathcal{L}$ provided by a belt with $M_{PL}=1\ M_\oplus$. Col. (4) is the solution to eq. (14); the mass doubling time for a planetesimal belt in the low-$\mathcal{L}$ regime is independent of the mass of the belt and also shorter for lower α. For small α, accretion onto planetesimals is faster, and the inner nebula quickly becomes more depleted. Asterisks indicate the high-$\mathcal{L}$ regime, in which eq. (14) is inapplicable.

is transient, because a certain amount of time is needed to reach steady state. At first, evaporated material is found only within a radial band of width ΔR (for water, $\Delta R \ll R$; Supulver & Lin 2000). This transient solution propagates toward the star and approaches a steady state only after a time $t_{ss}\sim R_{ev}/V_n \approx 1/(3\pi\alpha\eta)\approx 40/\alpha$ orbital periods. Of course, t_{ss} will also depend on Pr_t. For $R_{ev}=5$ AU, $\mathrm{Pr}_t=1$, and $\alpha=10^{-3}$ to 10^{-4}, $t_{ss}\sim 0.5$–5 Myr—long enough to be interesting for the chemistry of the early inner nebula (Cuzzi et al. 2003). Depending on the rate at which $\mathcal{L}$ grows, the nebula might evolve from regime 1 through regime 2 into regime 3 or directly from regime 1 into regime 3.

2.2. *Global Constraints on the Model*

Naturally, the steady state enhancement regime cannot persist for the entire duration of disk accretion. For example, in regime 2, with $E\sim 100$, as much water is accreting onto the star as hydrogen! This enhanced stage is limited in duration and intensity by (1) growth of the planetesimal sink at R_{ev}, leading to emergence of regime 3, and (2) depletion of the ultimate source of the enhancement, outer solar system solids.

In most nebula models, the surface mass density decreases as $1/R$. Thus, if the nebula extended only to 50 AU, 10 times farther than R_{ev}, and if *all* the solids in that region were to be carried into the region interior to R_{ev}, only an enhancement factor of 10 could be achieved; with $f_L<1$, the limit could be even lower. However, the true radial extent and mass distribution in the actual nebula are unknown; many protoplanetary disks are not tens but hundreds of AU across. Furthermore, some nebula models (e.g., Ruden & Pollack 1991) show the nebula surface mass density *increasing* outward, because of the effects of radially varying viscosity. In such a case, the same global constraint allows enhancement by a factor of 400, even if the nebula only extends to 50 AU. The likely time-variable nature of more realistic solutions should be kept in mind. Even while global source constraints limit the steady state solutions, large E_0 might prevail over limited times and radial distances. Improving astronomical observations of the radial extent and surface mass distribution of protoplanetary nebulae will be helpful in establishing such global constraints. Overall, we do not feel that values of $E_0\sim 10$–100 are unreasonable (especially in regime 1), but E_0 could be smaller (especially in regime 2) because of global constraints.

2.3. *The Sink: Planetesimal Growth outside the Condensation/Evaporation Boundary*

The sink term $\mathcal{L}$ removes solid material from further radial evolution by accreting it onto the surfaces of immobile planetesimals just outside R_{ev}. Thus, the local mass density of potential planet-forming objects increases. A detailed study of this process is well beyond the scope of this paper, but the following simple expressions illustrate the possibilities.

The mass lost to the planetesimal sink can be written as

$$\dot{M}_{PL}=2\pi R_{ev}EC_0\sigma_g V_n\mathcal{L}=\dot{M}EC_0\mathcal{L}. \tag{10}$$

Independently, we can write the mass accreted by a narrow belt of N_{PL} planetesimals with radius r_{PL} and total mass M_{PL} as

$$\dot{M}_{PL}=N_{PL}\pi r_{PL}^2\left(\frac{f_L EC_0\sigma_g}{h_L}\right)\Delta V\xi, \tag{11}$$

where $\Delta V\sim V_L\sim\eta V_K$ is the relative velocity of sweep-up, ξ is a sticking coefficient, and we have ignored gravitational focusing (appropriate for $r_{PL}<30$ km). Random velocities for meter-sized particles are comparable to V_g, so $h_L/H\sim(\alpha/\mathrm{Pr}_t)^{1/2}$ (Cuzzi & Hogan 2003; Cuzzi & Weidenschilling 2004). Setting equations (10) and (11) equal to each other, some algebra leads to

$$\mathcal{L}\approx\left(\frac{M_{PL}}{4\pi R_{ev}Hr_{PL}\rho_s}\right)\frac{\xi f_L\,\mathrm{Pr}_t^{1/2}}{\alpha^{3/2}}$$
$$\approx 2\times10^{-6}\xi\alpha^{-3/2}\left(\frac{M_{PL}}{M_\oplus}\right)\left(\frac{1\ \mathrm{km}}{r_{PL}}\right). \tag{12}$$

In evaluating equation (12) we assume $f_L=0.1$, $\rho_s=1$, $\mathrm{Pr}_t=1$, and $R_{ev}=5$ AU. Smaller bodies, which present a larger surface area for a given mass, are more efficient sinks provided that they are large enough to be immobile (greater than 100 m or so; the size is itself α-dependent). Without detailed accretion modeling, it is difficult to go further. However, at this level of description, interesting ranges of values for $\mathcal{L}$ and $\dot{M}_{PL}$ can be estimated (Table 1).

Equation (10) can be rewritten to estimate the planetesimal belt growth time (in orbital periods):

$$\frac{M_{\rm PL}}{\dot{M}_{\rm PL}} = \frac{M_{\rm PL}}{6\pi^2 R_{\rm ev}^2 E C_0 \sigma_g \eta \alpha \mathcal{L}} \approx \frac{2.4}{E\alpha\mathcal{L}} \left(\frac{M_{\rm PL}}{M_\oplus}\right) \approx 40 \left(\frac{M_{\rm PL}}{M_\oplus}\right)\left(\frac{1+\mathcal{L}}{\mathcal{L}}\right). \quad (13)$$

Equation (13) assumes a snow line at $R_{\rm ev} = 5$ AU, where $\sigma_g = 300$ g cm^{-2} and $C_0 = 0.01$. We used $E \sim E_0/(1+\mathcal{L})$ for $f_L \ll 1$ and equation (9) with $f_L = 0.1$.

In the $\mathcal{L} \ll 1$ regime, equation (13) can be combined with equation (12) to obtain a characteristic growth time for the belt (in orbital periods, shown in col. [4] of Table 1):

$$\frac{M_{\rm PL}}{\dot{M}_{\rm PL}}(\mathcal{L} \ll 1) \approx 2 \times 10^7 \alpha^{3/2} \xi^{-1} \left(\frac{r_{\rm PL}}{1\ {\rm km}}\right). \quad (14)$$

The transition from regime 2 to regime 3 can happen very quickly once nebular turbulence dies down (α decreases) near $R_{\rm ev}$; however, the poorly understood sticking coefficient ξ enters into all these timescales.

3. APPLICATIONS

3.1. *Meteoritics and Astronomical Observations*

Nebulae that are hot enough to evaporate silicates near the midplane in the terrestrial planet region ($\dot{M} \sim 10^{-7}\ M_\odot\ {\rm yr}^{-1}$ or age of $\sim 10^5$ yr; Bell et al. 1997) are probably also young enough that the drifting solids are more primitive and carbon-rich than chondrites. Evaporation of silicates in the presence of 20%–30% carbon by number may lead to the formation of abundant CO, with interesting mineralogical and isotopic implications (Cuzzi et al. 2003). For the duration of regime 1, this enhanced silicate and CO vapor plume near $R_{\rm ev}$(silicates) need *not* be accompanied by a similarly enhanced component of water, because the water stripped out of the drifting solids at $R_{\rm ev}$(water) remains at radii $\gg R_{\rm ev}$(silicates) until steady state is achieved some $t_{\rm ss} = 40/\alpha$ orbital periods later (regime 2). The potential duration of this dry, CO- and silicate-rich inner solar system regime 1 seems to be comfortably longer than the apparent duration of the calcium-aluminum–rich inclusion formation era in the inner solar system (Cuzzi et al. 2003), which plausibly ends when the inner nebula cools to below the evaporation temperature of common silicates, and thus long before the chondrule era that apparently occurs 1–3 Myr later (e.g., Amelin et al. 2002; Russell et al. 2004).

Before planetesimal growth at $R_{\rm ev}$(water) creates a sink, regimes 1 and 2 can provide an enhanced abundance of H_2O relative to hydrogen over a wide range of locations. This may help explain several aspects of chondrite chemistry indicative of elevated oxygen abundance, such as high levels of FeO in matrix olivines in both ordinary and carbonaceous chondrites (Nagahara 1984; Scott et al. 1984, 1988; Wood 1988). It has traditionally been argued that enhancement of nebula gas in silicates of chondritic composition can provide the high oxygen fugacity required for high-FeO silicates to form in the nebula (Palme & Fegley 1990). Recently, however, Fedkin & Grossman (2004) have shown that chondritic silicates are ineffective in this regard because they provide too much sulfur (which competes for iron) in addition to their oxygen. Our mechanism enriches the nebula gas in H_2O alone and might provide the needed oxygen fugacity without the sulfur complications. In another application, Ciesla et al. (2003) have suggested that fine-grained silicates can be aqueously altered in the nebula *gas* by shock waves, if the nebula gas is enhanced in H_2O by something like a factor of 100. This level of enhancement is achievable, even if perhaps only regionally or for a limited time, under circumstances described here. Furthermore, the enhancement is probably temporally and spatially variable, depending on how the nebula evolves between the three regimes we have identified. In addition, A. Krot (2004, private communication), pointed out to us that this enhancement mechanism can affect the oxygen isotopic ratios in primitive meteorite minerals in a time-variable way, if outer solar system ice has different O-isotopic composition from inner solar system silicates (e.g., Lyons & Young 2004; Yurimoto & Kuramoto 2004; A. Krot et al. 2004, in preparation).

Some recent astronomical observations seem to show abundant CO in the terrestrial planet regions of vigorously accreting protoplanetary nebulae (Najita et al. 2003). The presence of abundant CO might be associated with the evaporation front of primitive silicate-carbon material discussed above. In at least one case, the water content in the inner nebula seems to be low relative to CO (Carr et al. 2004). This could be the signature of regime 1 or perhaps a very early stage regime 3. Future observations of this type, perhaps at higher spatial resolution, might help us determine evolutionary timescales and connect the current properties of external protoplanetary nebulae with the record of the accretion process in our own.

3.2. *Planetary Formation*

The formation of Jupiter has long been associated with the concept of a snow line (Wuchterl et al. 2000). The nominal scenario for the formation of an icy Jovian core in less than a few million years, while the nebula gas is still present, requires that the surface mass density of solids in the formation region exceed that of a minimum mass nebula by almost an order of magnitude (Lissauer 1987). One well-known proposal for this enhancement is the cold finger effect, in which the entire water content of the *inner* nebula is diffusively transported to the snow line and frozen out there (Stevenson & Lunine 1988). With the assumptions of a vigorously turbulent inner nebula, a narrow condensation annulus, and no leakage back into the inner solar system (questioned by Sears 1993), the cold finger effect leads to an enhancement of solids outside the snow line by a factor of 6–25 in about 10^5 yr. This can be expressed as a mass flux of roughly $\pi R_{\rm ev}^2 C_0 \sigma_g / (R_{\rm ev}^2/\mathcal{D}) \sim \pi C_0 \sigma_g \mathcal{D} \sim$ a few times $10^{-5}\ M_\oplus\ {\rm yr}^{-1}$ for ${\rm Pr}_t \sim 1$. The ratio of the mass flux to $R_{\rm ev}$ due to solids drifting from *outer* regions (this paper) to that due to solar abundance vapor diffusing from the *inner* solar system is

$$\frac{2\pi R_{\rm ev} f_L C_0 \sigma_g V_L}{\pi C_0 \sigma_g \mathcal{D}} = \frac{2 R_{\rm ev} f_L V_L}{\mathcal{D}} \approx 3 E_0\ {\rm Pr}_t \approx \frac{2 f_L}{(\alpha/{\rm Pr}_t)}. \quad (15)$$

Unless the turbulent Prandtl number is very small, i.e., unless turbulent transport is much larger than viscous transport, and given the validity of our particle size distribution arguments, inward particle drift and vapor retention would seem to be the dominant source for enhancement of solids near $R_{\rm ev}$.

Looking somewhat further beyond the boundaries of this paper, we suspect that evaporation fronts of low-temperature volatiles might also have important implications for their enhancement in the gaseous envelope of Jupiter, a problem

highlighted by Owen et al. (1999) and Atreya et al. (2003). Another possibility, associated with R_{ev}(silicates), is the isotopic homogenization of a large amount of the silicate material that ultimately ends up in meteorite parent bodies. The gross isotopic homogeneity of meteoritic silicates has been a persistent puzzle, because few nebula models evaporate silicates throughout the asteroid formation region. It has also been suggested to us (J. Chambers 2003, private communication) that the process, operating at R_{ev}(silicates), might help explain the mass distribution in the terrestrial planet formation region. Some of these applications will be addressed in future papers.

4. SUMMARY

We show that nebula constituents will be enhanced in the vicinity of their condensation/evaporation boundaries R_{ev}, because of rapid inward drift of solid material in the form of meter-sized boulders and slow subsequent removal of the ensuing vapor. This *evaporation front* effect modifies not only the surface mass density of solids available just *outside* R_{ev} (useful for planet building) but also the chemistry and mineralogy of material that resides well *inside* R_{ev} (of potential importance to meteoritics and gas giant atmospheres). The enhancements can be 1 or even 2 orders of magnitude and probably vary on timescales of a million years or so—perhaps also exhibiting significant radial variation during that time. Some of these properties might be observable by astronomical observations.

We thank Stu Weidenschilling and Robbins Bell for helpful conversations during the course of this research. We thank Lynne Hillenbrand for drawing our attention to the astrophysical observations and Joan Najita and John Carr for helpful discussions and preprints in advance of publication. We thank Larry Grossman for discussions regarding the applicability to meteoritic silicates and John Chambers for the suggestion that there may be an application to mass densities in the terrestrial planet region. We thank Jack Lissauer and John Chambers for reviews of an early draft. We thank Rich Young for bringing the Jovian volatiles problem to our attention. We thank our reviewer, David Stevenson, for useful suggestions on presenting caveats. This research was supported by a grant to J. N. C. from NASA's Origins of Solar Systems program and a grant to K. J. Z. from NASA's Exobiology program.

REFERENCES

Amelin, Y., Krot, A. N., Hutcheon, I. D., & Ulyanov, A. A. 2002, Science, 297, 1678
Atreya, S. K., Mahaffy, P. R., Niemann, H. B., Wong, M. H., & Owen, T. C. 2003, Planet. Space Sci., 51, 105
Bell, K. R., Cassen, P. M., Klahr, H. H., & Henning, T. 1997, ApJ, 486, 372
Calvet, N., Hartmann, L., & Strom, S. E. 2000, in Protostars and Planets IV, ed. V. Mannings, A. P. Boss, & S. S. Russell (Tucson: Univ. Arizona Press), 377
Carr, J. S., Tokunaga, A. T., & Najita, J. 2004, ApJ, 603, 213
Ciesla, F., Lauretta, D. S., Cohen, B. A., & Hood, L. L. 2003, Science, 299, 549
Cuzzi, J. N., Davis, S. S., & Dobrovolskis, A. R. 2003, Icarus, 166, 385
Cuzzi, J. N., Dobrovolskis, A. R., & Champney, J. M. 1993, Icarus, 106, 102
Cuzzi, J. N., & Hogan, R. C. 2003, Icarus, 164, 127
Cuzzi, J. N., Hogan, R. C., Paque, J. M., & Dobrovolskis, A. R. 2001, ApJ, 546, 496
Cuzzi, J. N., & Weidenschilling, S. J. 2004, in Meteorites and the Early Solar System II, ed. D. Lauretta, L. A. Leshin, & H. Y. McSween, Jr. (Tucson: Univ. Arizona Press), submitted
Cyr, K., Sears, W. D., & Lunine, J. I. 1998, Icarus, 135, 537
Dubrulle, B., Morfill, G. E., & Sterzik, M. 1995, Icarus, 114, 237
Fedkin, A. V., & Grossman, L. 2004, in 35th Lunar and Planetary Science Conf. (Houston: LPI), abstract 1823
Lissauer, J. J. 1987, Icarus, 69, 249
Lyons, J. R., & Young, E. D. 2004, in 35th Lunar and Planetary Science Conf. (Houston: LPI), abstract 1970
Morfill, G. E., & Völk, H. J. 1984, ApJ, 287, 371
Nagahara, H. 1984, Geochim. Cosmochim. Acta, 48, 2581
Najita, J., Carr, J. S., & Mathieu, R. D. 2003, ApJ, 589, 931
Nakagawa, Y., Sekiya, M., & Hayashi, C. 1986, Icarus, 67, 375
Owen, T., Mahaffy, P., Niemann, H. B., Atreya, S., Donahue, T., Bar-Nun, A. & de Pater, I. 1999, Nature, 402, 269
Palme, H., & Fegley, B. 1990, Earth Planet. Sci. Lett., 101, 180
Prinn, R. G. 1990, ApJ, 348, 725
Ruden, S., & Pollack, J. B. 1991, ApJ, 375, 740
Russell, S. S., Hartmann, L., Cuzzi, J., Krot, A. N., Gounelle, M., & Weidenschilling, S. 2004, in Meteorites and the Early Solar System II, ed. D. Lauretta, L. A. Leshin, & H. Y. McSween, Jr. (Tucson: Univ. Arizona Press), submitted
Scott, E. R. D., Barber, D. J., Alexander, C. M., Hutchison, R., & Peck, J. A. 1988, in Meteorites and the Early Solar System, ed. J. F. Kerridge & M. S. Matthews (Tucson: Univ. Arizona Press), 718
Scott, E. R. D., Rubin, A. E., Taylor, G. J., & Keil, K. 1984, Geochim. Cosmochim. Acta, 48, 1741
Sears, W. D. 1993, in 24th Lunar and Planetary Science Conf. (Houston: LPI), 1271
Sirono, S., & Greenberg, J. M. 2000, Icarus, 145, 230
Stepinski, T. F. 1998, Icarus, 132, 100
Stepinski, T. F., & Valageas, P. 1997, A&A, 319, 1007
Stevenson, D. J., & Lunine, J. I. 1988, Icarus, 75, 146
Stone, J. M., Gammie, C. F., Balbus, S. A., & Hawley, J. F. 2000, in Protostars and Planets IV, ed. V. Mannings, A. P. Boss, & S. S. Russell (Tucson: Univ. Arizona Press), 589
Supulver, K., & Lin, D. N. C. 2000, Icarus, 146, 525
Weidenschilling, S. J. 1977, MNRAS, 180, 57
———. 1997, Icarus, 127, 290
———. 2000, Space Sci. Rev., 92, 295
Weidenschilling, S. J., & Cuzzi, J. N. 1993, in Protostars and Planets III, ed. E. Levy & J. Lunine (Tucson: Univ. Arizona Press), 1031
Wood, J. A. 1988, Annu. Rev. Earth Planet. Sci., 16, 53
Woolum, D., & Cassen, P. M. 1999, Meteoritics Planet. Sci., 34, 897
Wuchterl, G., Guillot, T., & Lissauer, J. J. 2000, in Protostars and Planets IV, ed. V. Mannings, A. P. Boss, & S. S. Russell (Tucson: Univ. Arizona Press), 1081
Yurimoto, H., & Kuramoto, K. 2004, Science, in press